# Lattice dynamics and stability of modulated-strain structures for elastic phase transitions in alloys

J. Pouget
*Laboratoire de Modélisation en Mécanique, Université Pierre et Marie Curie, 4 Place Jussieu, 75252 Paris CEDEX 05, France*
(Received 2 February 1993)

In this paper we intend to discuss in detail the question of an instability process of modulated-strain structures in alloys that undergo a first-order phase transformation. In addition, we aim at characterizing the formation of nonlinear structures in the pretransformation regime produced by the instability mechanism. The model is based on a two-dimensional lattice including nonlinear and competing interactions, which play a key role in the instability of a homogeneous solution. Although the main body of the study is devoted to the nonlinear dynamics of a lattice model, an excursion in linear analysis provides us with necessary results about the critical behavior of the system. Indeed, the linear problem leads us to the study of the phonon-dispersion branch, and the existence of a critical point of the phonon-dispersion curve is then shown for a particular value of the elastic coefficient (here, the control parameter of the phase transition). This critical behavior is, in fact, related to the softening of the dispersion curve at a nonzero wave number. The nonlinear analysis becomes essential when the system is linearly unstable in the vicinity of the critical point. An amplitude equation of the Ginzburg-Landau type is next deduced in a semidiscrete approach by using a multiple-scale technique. The examination of the stability of steady solutions allows one to determine the nature of the bifurcation near the critical point. The study of the bifurcating stationary solutions shows an instability process for long-wavelength modulations taking place in the transverse direction of the two-dimensional system. The mechanism of self-generated nonlinear structures in the two-dimensional lattice near the critical region of the phonon dispersion is numerically investigated. Nontrivial localized structures are then demonstrated. By way of conclusion, some emphasis is placed on the pretransformation phenomena in martensitic materials or ferroelastic crystals.

## I. INTRODUCTION

A lot of interest has recently been devoted to spatiotemporal patterns as well as the associated defects and dynamics such as standing-wave patterns, localized structures including solitons or oscillating patterns. These structures become fundamental in the study of phase transitions which are usually accompanied by the appearance of defects: dislocation motions, grain boundaries, domain wall structures, and twinnings.[1–3] The present paper is particularly motivated by the pretransformation structures occurring in phase transformations in crystalline alloys. More precisely, we are interested in strain structures for martensitic-ferroelastic transformations which are described by a strain order parameter including a displacive first-order phase transition.[4–6] Pretransitional effects can be seen as a martensitic phase partially developed in the parent phase and this is characterized by modulated structures or strain modulations. These structures made of spatially periodic arrangements of martensites are referred to as "tweed patterns" occurring in a wide range of temperature followed at lower temperature by the martensitic transformation. Moreover, the dynamics of martensitic twinning turns out to be important for phase transformation and can be considered as a nucleation and growth mechanism of martensitic embryos. On the other hand, we propose here to illustrate complex spatiotemporal patterns in the context of phase transformations in solids. Such problems are more commonly met in the framework of hydrodynamical systems, chemical reactions, or crystal growth.[7–9] One of the essential aims of the work is to understand how instabilities arising at the microscale, that is, at the level of the lattice model, are able to organize the system at the macroscale and what the selection properties of the nonlinear structures are.

The physical implications of the proposed lattice model lie in the existence of lattice instability which manifests itself by the existence of low-lying transverse-acoustic phonons propagating along the [110] direction of the cubic lattice. The instability exhibits strain modulation or modulated domains and microstructures occurring in some range of temperature and then followed at lower temperatures by the martensitic transformation.[6,10–12] These microstructures are viewed as strain embryos of martensitic phase. Alloys such as Ni-Al, Zr-Nb, Ti-Ni, and others suffer this kind of instability with a condensation of their acoustic phonons producing a low value of the corresponding shear elastic constant and this has been observed by means of neutron scattering experiments. It is now well established that this anomalous change in the elastic behavior and phonon spectra is precursory to the oncoming displacive phase change. High-resolution electron microscopy has revealed microstructures made of fine-scale arrangements of modulated-strain domains.[13,14] We propose here an alternative view to attempt to understand the formation of such microstructures in terms of lattice instability and spatiotem-

0163-1829/93/48(2)/864(12)/$06.00  

poral structures.

We confine our attention to the stability of modulated-strain structures or lattice-distortion waves on the basis of a two-dimensional lattice model. The standpoint of the study is then a lattice plane involving competing and nonlinear interactions which are the key ingredients to describe the relevant phenomena. The same lattice model has been used to examine with success the formation of localized strain patterns decaying in all directions.[15–17] The important and interesting results provided by the study of the model are (i) the partial softening of the transverse-acoustic phonon branch at a nonzero wave number, (ii) the positive curvature of the dispersion branch at the long-wavelength limit,[16–19] and (iii) the shearing motion of the atomic planes along the stacking direction leading to spatially arranged structures made of martensitic twin bands and the existence of strain solitary waves describing the coherent movement of martensitic domains.[16–19] The nonlinear dynamics of the two-dimensional system has allowed us to examine the stability of the lattice and numerical simulations have shown the formation of localized strain structures emerging from an instability mechanism.[16,17] In the present paper we continue the investigation of the properties of our lattice model when the formation of elastic structure deals with steady state of periodic strain patterns. The study is physically concerned with pretransitional effects in phase transformations and the description of microtwinning formation emerging from a lattice instability. The first essential step toward the understanding of the mechanism responsible for the new pattern formation is the linear analysis of the lattice stability. Then we determine the critical conditions for the onset of the instability from the softening of the acoustic-phonon branch which occurs at a nonzero wave number.[20,22] The study provides also the critical wave number or wavelength for which instability disturbances are most likely to grow first. The instability mechanism is, in fact, controlled by a parameter which is just the elastic constant. However, as this control parameter is decreased below a certain critical value, the initially small perturbations grow with time until they are so large that the nonlinear terms become significant and prevent the unlimited growth of perturbations. The produced nonlinear structures that take place in the system are the result of the competition between the linear amplification and nonlinear saturation. Consequently, the pattern selection mechanisms which are produced by the competing process are strongly dependent on the implication of the nonlinearities of the system, in particular in the postbifurcation regime. In order to obtain some useful information about the nonlinear analysis we must take the advantage of a perturbative method. The way of developing a perturbative scheme turns out to be efficient by examining the situation near the instability point. Then, from rather complicated dynamical equations for the discrete system (microscopic model) we derive an amplitude equation that describes the nonlinear dynamics near the critical point. The equation thus obtained is similar to that of Ginzburg-Landau type. The study of this model equation allows us to define a criterion of stability for modulated-strain structures and the nature of the instabilities as well as the pattern formation thus produced are checked by means of numerical simulations. The latter are in good agreement with the physical conjectures and show the organization of the system beyond the instability regime.

The paper is organized as follows. In the next section, Sec. II, the lattice model is briefly recalled and the equations of motion for the discrete system are given. The linear analysis of the discrete system is presented in Sec. III. In this section, we point out the possible softening of the acoustic-phonon branch at a nonzero wave number due to the introduction of competing interactions at the microscopic scale. Then, the existence of a critical point for the dispersion phonon is proved, which gives rise to the lattice instability. In Sec. IV we use a perturbative scheme based on multiple-scale technique in order to derive an amplitude equation which governs the dynamics of the system near the critical point. Moreover, this amplitude equation is obtained in a semidiscrete approach, which makes the instability analysis particularly interesting and powerful. The instability of a modulated-strain structure is analyzed in detail in Sec. V and some physical implications are given. The problem is then illustrated by means of numerical experiments exhibiting rather complex localized patterns emerging from the instability process. We conclude the paper in Sec. VI by saying a few words on the relationship between the pattern formation and the transformation and some further extensions of the model are evoked.

## II. THE MODEL AND EQUATIONS OF MOTION

### A. Construction of the model

We give here, very briefly, the main features of the lattice model; for more details the reader must be referred to Ref. 17. Let us consider a lattice plane extracted, for instance, from a cubic structure (the high-temperature phase, untransformed lattice) made of squares parallel to the $i$ and $j$ directions (see Fig. 1 of Ref. 17). A lattice point of the plane is located by $(i,j)$. Each particle of the lattice can move in the plane and we denote by $u(i,j)$ and $v(i,j)$ the displacements in the $i$ and $j$ directions, respectively. Along with Ref. 17, we consider a particular transformation described by the displacement $u$ only. We next introduce discrete deformations defined by

$$S(i,j)=u(i,j)-u(i-1,j)\ , \tag{1a}$$

$$G(i,j)=u(i,j)-u(i,j-1)\ . \tag{1b}$$

The first strain (1a) represents the elongational deformation in the direction $i$ and Eq. (1b) denotes a pure shear.

### B. The lattice energy

Insofar as the interatomic interactions are concerned, we assume that the particles interact via two types of interatomic potential. The first kind of interactions is supposed to be a function of particle pairs between the first-nearest neighbors in the $i$ and $j$ directions. The potential describing these interactions must possess stable, unsta-

ble, or metastable states according to a control parameter (which can be connected with temperature).[10] The second kind of interatomic interactions is suppose to model the resistance of the crystalline cell to twisting and bending due to the long-range atomic interactions.[16,18] These interactions involve noncentral forces and are called three-body interactions. Moreover, they occur between first- and second-nearest neighbors. The noncentral interactions are of particular interest for the competing interactions and stability of the nonlinear structures. On using the invariances of the lattice energy under translations and rotations,[17] we can adopt the following functional:

$$\mathcal{V}=\sum_{(i,j)}[\Phi(S(i,j))+\tfrac{1}{2}\beta[G(i,j)]^2+\tfrac{1}{2}\delta\{[\Delta_L^+S(i,j)]^2+[\Delta_T^+G(i,j)]^2\}$$
$$+\tfrac{1}{2}\eta(\{\Delta_L^+[S(i+1,j)+2S(i,j)+S(i-1,j)]\}^2+\{\Delta_T^+[G(i,j+1)+2G(i,j)+G(i,j-1)]\}^2)] , \quad (2)$$

where the potential $\Phi$ is given by

$$\Phi(S)=\tfrac{1}{2}\alpha S^2-\tfrac{1}{3}S^3+\tfrac{1}{4}S^4 . \quad (3)$$

The lattice energy (2) has been written in dimensionless units for ease of presentation. The first and second terms in Eq. (2) represent the linear and nonlinear potentials coming from the particle pair interactions where $\alpha$ and $\beta$ are the lattice force coefficients for the longitudinal and shear deformations, respectively. The third and fourth parts of the lattice energy (2) hold for the actions of the noncentral interactions in the $i$ and $j$ directions. The interactions are characterized by the parameters $\delta$ and $\eta$ for the actions between first- and second-nearest particles, respectively. On the other hand, the operators $\Delta_L^+$ and $\Delta_T^+$ hold for the forward first-order finite differences in the $i$ and $j$ directions $[\Delta_L^+f(i,j)=f(i+1,j)-f(i,j)$ and $\Delta_T^+f(i,j)=f(i,j+1)-f(i,j)]$. We notice that, thanks to Eqs. (1a) and (1b), the noncentral interactions in Eq. (2) can be written in the form $u(i-1,j)-2u(i,j)+u(i+1,j)$ for the first-nearest-neighbor interaction and $u(i-2,j)-2u(i,j)+u(i+2,j)$ for the second-nearest-neighbor interaction; the same holds true in the $j$ direction for the deformation $G(i,j)$. A one-dimensional model can be extracted from the complete two-dimensional system. This one-dimensional model thus reduced has been examined in detail and it has allowed us to model localized structures made of arrays of elastic solitary waves.[16,19]

### C. Equations of motion

Let us introduce the kinetic energy associated with the displacement $u$,

$$K=\sum_{(i,j)}\tfrac{1}{2}\dot{u}^2(i,j) , \quad (4)$$

the mass of the particles has been set to unit. Then, a set of equations of motion for the displacement $u$ can be deduced from the Hamiltonian $K+\mathcal{V}$. On accounting for Eqs. (1a) and (1b) the equations of motion can be written in terms of the discrete deformation $S(i,j)$,

$$\ddot{S}(i,j)+\Gamma\dot{S}(i,j)=\Delta_L^2\Sigma_L(i,j)+\Delta_T^2\Sigma_T(i,j) , \quad (5)$$

where we have set

$$\Sigma_L(i,j)=\sigma(i,j)-\Delta_L^-\chi_L(i,j) , \quad (6a)$$

$$\Sigma_T(i,j)=\beta S(i,j)-\Delta_T^-\chi_T(i,j) , \quad (6b)$$

$$\sigma(i,j)=\alpha S(i,j)-S^2(i,j)+S^3(i,j) , \quad (6c)$$

$$\chi_L(i,j)=\Delta_L^+\{\delta S(i,j)+\eta[S(i+2,j)+4S(i+1,j)+6S(i,j)+4S(i-1,j)+S(i-2,j)]\} , \quad (6d)$$

$$\chi_T(i,j)=\Delta_T^+\{\delta S(i,j)+\eta[S(i,j+2)+4S(i,j+1)+6S(i,j)+4S(i,j-1)+S(i,j-2)]\} . \quad (6e)$$

The operators $\Delta_L^-$ and $\Delta_T^-$ represent the backward first-order finite differences in the $i$ and $j$ directions, respectively. Next, $\Delta_L^2$ and $\Delta_T^2$ denote the second-order finite differences in the $i$ and $j$ directions, as well. Furthermore, a damping effect characterized by $\Gamma$ has been accounted for. In Eq. (5), macroscopic stresses are defined by the first part of Eqs. (6a) and (6b) and microscopic stresses due to the noncentral interactions are given by Eqs. (6d) and (6e). We remark that the stress defined by Eq. (6c) is a nonlinear function of the discrete strain $S$. The set of nonlinear difference-differential equations (5) governs the deformation $S$. Nevertheless, because of the strongly nonlinear nature of the problem, these equations are not manageable except for the linear problem which will be examined in the next section. The set of nonlinear discrete equations (5) can be solved, of course, by means of numerical simulations with appropriate initial and boundary conditions. However, an alternative situation occurs in the case of the continuum approximation. This situation leads to the quasi-continuum model including the leading discreteness effects and this quasi-continuum model has allowed us to study the problem of the formation of spatially localized structures and their stability. This problem has been presented in detail in another work[16,17] and has provided important physical situations concerning the elastic domain formation for phase transformations in alloys including martensitic materials.

In the present work, the emphasis is placed especially on the nonlinear dynamics of modulated-strain structures and the possible nonlinear structure formation. The state of deformation is determined by the linear problem whose wavelength corresponds to the critical point of the acoustic-phonon branch at a nonzero wave number. Accordingly, a semidiscrete approach turns out to be quite necessary to arrive at a more realistic mechanism for pattern formation.

## III. LINEAR ANALYSIS

The linear analysis of the model is nonetheless particularly important since it informs us about the linear stability of the basic solution of a uniformly deformed lattice. We consider the linearized equations (5) about a uniform deformation $S_0$. The latter is, however, chosen in order to correspond to one of the stable minima of the lattice potential (3). Then, we have two cases: $S_0=0$ (austenitic phase) or $S_0\neq 0$ (martensitic phase) according to the parameter $\alpha$.[18] Since we are concerned with the linear problem we look for solutions to the linearized equations (5) as traveling harmonic plane waves in the $i$ direction only, this leads to the dispersion relation relating the circular frequency to $p$ the wave number ($p\in[0,\pi]$),

$$\omega^2+i\Gamma\omega=\omega_0^2(p)\ , \tag{7a}$$

with

$$\omega_0^2(p)=4\left[\hat{\alpha}(S_0)\sin^2\left[\frac{p}{2}\right]+4\delta\sin^4\left[\frac{p}{2}\right]+\eta\sin^4(p)\right]\ , \tag{7b}$$

where we have set

$$\hat{\alpha}(S_0)=\alpha-2S_0+3S_0^2=\left[\frac{d^2\Phi}{dS^2}\right]_{S=S_0}\ . \tag{8}$$

Equation (8) represents the induced elastic modulus in the martensitic phase if $S_0\neq 0$ or in the austenitic phase if $S_0=0$. The dispersion relation (7) for $\Gamma=0$ is shown in Fig. 1 for different values of the parameter $\alpha$, $\delta$, and $\eta$. According to the relative values of these parameters, the competing interactions (interactions by pairs and noncentral forces) are of great interest and this exhibits particularly important physical situations. Curve (a) differs slightly from the classical acoustic branch of the bare monatomic chain. Curve (b) leads, in fact, to a dispersion branch with an upward convexity at the long-wavelength region. This is possible if the condition

$$\alpha(S_0)/12-(\delta+16\eta)<0 \tag{9}$$

is met. Moreover, this condition has turned out to be crucial for the existence of strain solitary waves.[19] The dispersion branch (c) has a small dip at a nonzero wave number and the acoustic-phonon branch undergoes a softening at this wave number which can be interpreted as precursor of a martensitic transformation. At length, curve (d) corresponds to the critical situation for which we have

$$\omega_0^2(p_0,\alpha_0)=0 \quad \text{and} \quad \frac{d}{dp}\omega_0^2(p,\alpha)\bigg|_{(p_0,\alpha_0)}=0\ . \tag{10}$$

The stability of the linear modes is provided by the condition $\mathrm{Im}(\omega_\pm)<0$ for all $p$'s, where $\omega_\pm$ are the two roots of Eq. (7a) for $\Gamma\neq 0$. Conversely, it is unstable if there is at least one value of $p$ for which $\mathrm{Im}(\omega_\pm)>0$. In fact, $\mathrm{Im}(\omega_-)<0$ holds true for all $p$'s. Therefore the imaginary part of $\omega_+$ is positive if $\omega_0^2<0$ and for this case, the unstable mode is $\omega_+=-i(\frac{1}{2}\Gamma-\sqrt{\Gamma^2/4-\omega_0^2})$. The critical point is such that $\omega_+=0$ and $d\omega_+/dp=0$; these conditions are quite equivalent to those given by Eq. (10). The details of the curve $\mathrm{Im}(\omega_+)$ as a function of $p$ ($p\in[0,\pi/2]$) around the critical point are shown in Fig. 2 when the parameter $\alpha$ is varied above and below the critical point. Curve (a) depicts the damped harmonic mode traveling on a classical atomic chain. Curve (b) corresponds to the stable case since $\alpha>\alpha_0$, hence $\mathrm{Im}(\omega_+)<0$. The critical case is plotted in curve (c) for which the conditions (10) are fulfilled and the curve is tangent to the $p$ axis. Curve (d) has a segment of $p$ where the system is linearly unstable since $\mathrm{Im}(\omega_+)>0$ on this segment.

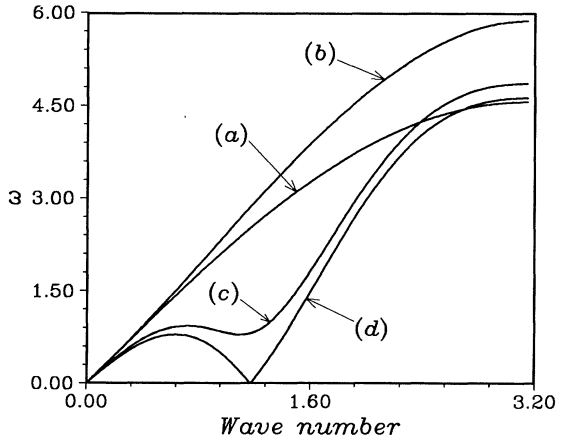


FIG. 1. Dispersion curves of the acoustic phonons. (a) the classical one-dimensional monatomic chain, (b) curve with an upward convexity at the long-wavelength limit, (c) dispersion branch with a small dip for $\alpha>\alpha_0$, and (d) dispersion branch passing through the critical point at $p_0$ for $\alpha=\alpha_0$.

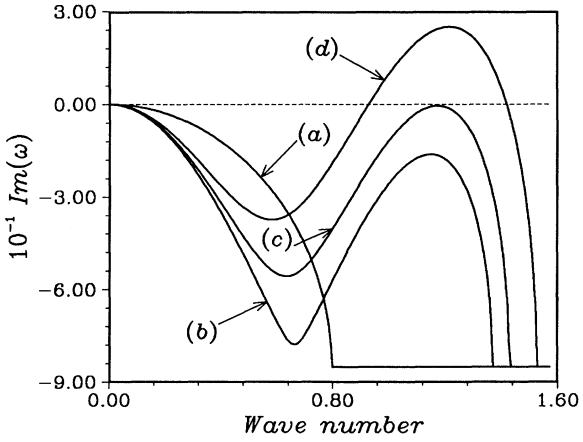


FIG. 2. Imaginary part of the frequency spectrum as a function of the wave number $p$ in the vicinity of the critical point. (a) The classical case: damped monatomic chain, (b) stable case $\alpha>\alpha_0$, (c) the critical case for $p=p_0$ and $\alpha=\alpha_0$, and (d) for $\alpha<\alpha_0$ there exists a small segment where the lattice is linearly unstable.

The critical situation occurs when $\omega_0^2$ vanishes for a particular nonzero value of $p$, say $p_0$, while $\omega_0^2$ remains positive for all other $p$'s. This situation is obtained, of course, by an appropriate choice of the control parameter $\alpha$ which is the elastic modulus of the lattice. Then $\alpha=\alpha_0$ denotes the critical value of the control parameter for which a periodic state of strain with the wave number $p_0$ takes place in the lattice. The values $p_0$ and $\alpha_0$ are therefore such that $p_0$ is a double root of $\omega_0^2$ [double root of Eq. (7a), as well] and must check the condition (10). The other roots remain always negative. We now use the dispersion relation (7b) and the condition (10) to determine the wave number of the critical point. We find then

$$\sin^2\left[\frac{p_0}{2}\right]=\frac{(2-\sqrt{1-3\delta/16\eta})}{3}\ , \tag{11a}$$

$$\alpha_0=-128\eta\sin^4\left[\frac{p_0}{2}\right]\cos^2\left[\frac{p_0}{2}\right]\ . \tag{11b}$$

The solution (11a) exists if, first of all, $\alpha_0>0$, hence $\eta<0$. Second, the right-hand side of Eq. (11a) must be positive and smaller than one, and third, we consider the situation where $p_0$ is the only root of the dispersion relation. These conditions imply that $0\le p_0\le\pi/2$ and $-16<\delta/\eta<4$. Figure 3 shows the critical wave number $p_0$ as a function of the ratio $\delta/\eta$. The variation of the critical elastic modulus versus $p_0$ is given in Fig. 4.

Such a softening effect is usually observed by neutron scattering technique.[23–25] In fact, precursor structures occur and are characterized by modulated lattice distortion within the high-temperature phase and electron micrographs exhibit fine-scale, diffuse, striation microstructures which are commonly referred to as "tweed patterns."[26,27]

## IV. NONLINEAR ANALYSIS

The linear theory tells us that unstable perturbations with wave numbers lying on a segment around $p_0$ will be growing drastically as time elapses. The linear approximation therefore breaks down after a time of the order $1/\omega$ and the nonlinear terms would no longer be ignored. With the view of examining the influence of nonlinearities on structure stability we adopt the so-called multiple-scale technique which is a common method used in hydrodynamical systems and dissipative structures.[7,28–31] The first step of the task is to specify how characteristic time and length scales appear near the bifurcation point $(\alpha_0,p_0)$. Then, we expand $\omega$ to the leading order in the neighborhood of the critical point; we have

$$\omega_+\simeq-\frac{i}{\Gamma}\left\{4\sin^2\left[\frac{p_0}{2}\right](\alpha-\alpha_0)+64\sin^2\left[\frac{p_0}{2}\right]\left[\frac{d^2\omega^2}{d[4\sin^2(p/2)]^2}\right]_{p=p_0}\times\left[\sin\left[\frac{p}{2}\right]-\sin\left[\frac{p_0}{2}\right]\right]^2\right\}\ . \tag{12}$$

It follows from Eq. (12) that the range of wave number near $p=p_0$ for which the homogeneous periodic structure is unstable is then $\Delta p\simeq F(p_0)(\alpha_0-\alpha)^{1/2}$ where $F$ is a function of $p_0$ that we do not write. The corresponding length scale for modulations of the structure that can be considered with this band of wave number is $\Delta l=1/\Delta p$, which is large in comparison with the original wavelength $2\pi/p_0$ (scale separation). Moreover, since $\omega\propto(\alpha-\alpha_0)$ for the corresponding modulation modes, the characteristic time scale of the interesting modulation is of order $(\alpha-\alpha_0)^{-1}$. The procedure of the multiple-scale method is to attempt to separate the fast variations in space and time from the slow ones. We introduce now a small parameter as follows:

$$\alpha=\alpha_0+\lambda\epsilon^2\ . \tag{13}$$

Nevertheless, since the basic linear analysis which has led us to the dispersion relation has been obtained for the discrete system, we must, as far as possible, keep the most leading feature of the discrete problem. Such a study is

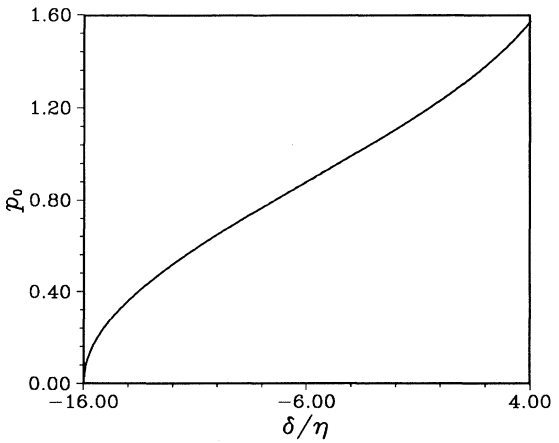


FIG. 3. The critical wave number as a function of the ratio $\delta/\eta$ on the segment $[-16,4]$.

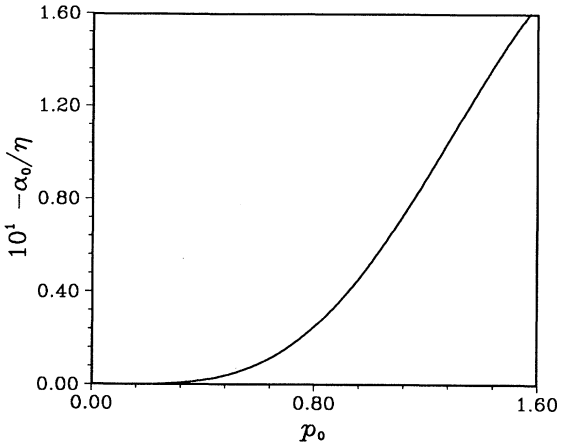


FIG. 4. The critical elastic modulus $\alpha_0$ as a function of the critical wave number $p_0$ ($p_0\in[0,\pi/2]$).

usually not tractable and accordingly we adopt a semidiscrete analysis. The method consists in separating the fast changes of the periodic structure involving the discrete phase $np_0$ while the amplitude part will be treated in the continuum limit.[32,33] Then, we start with an asymptotic series of $S(n,m)$ in $\epsilon$ and in harmonics of the phase variable

$$S(n,m)=\epsilon A(n,m)e^{inp_0} +\epsilon^2 l[B_1(n,m)e^{inp_0}+B_2(n,m)e^{2inp_0}]+\text{c.c.} \tag{14}$$

The time variable has been omitted for ease of presentation, but $A$, $B_1$, and $B_2$ are also functions of time. The procedure is now to substitute (14) into Eqs. (5) and (6a)–(6e) and equate powers of $\epsilon$ up to the third order for the same harmonic. In fact, the expression (14) is just the solution needed to determine the appropriate solution to the first order. On assuming slowly varying envelopes $A$, $B_1$, and $B_2$ in space we can consider the continuum approximation for these functions while we take finite differences of the phase for the discrete variable. We introduce, next, for the envelope the slow time variable $\tau=\epsilon^2 t$ and space variables $X=\epsilon x$ and $Y=\epsilon y$ where the small parameter $\epsilon$ corresponds, of course, to the order of the characteristic space and time scales. First of all, at the first order in $\epsilon$ of the harmonic one, we recover the condition $\omega_0^2(p_0,\alpha_0)=0$. Secondly at the next order (i.e., $\epsilon^2$) of the same harmonic, we have again $(d\omega_0^2/dp)_{p=p_0}=0$. The third order provides then the equation for the envelope $A$ coupled to $B_2$. Now by equating the second harmonic according to the power in $\epsilon$ we reach two relationships between $B_2$ and $A$, and $B_1$ and $A$ next. Without dwelling on algebraic manipulations but by using straightforward computation, we arrive finally at

$$\Gamma A_\tau-(\omega^2)_{pp}A_{XX}-\beta A_{YY}+\bar{\lambda}A-\mu|A|^2A=0\ , \tag{15a}$$

where we have defined

$$(\omega^2)_{pp}=\left[\frac{d^2\omega_0^2}{dp^2}\right]_{p=p_0}\ , \tag{15b}$$

$$\bar{\lambda}=4\lambda\sin^2(p_0/2)\ , \tag{15c}$$

$$\mu=4\sin^2(p_0/2)\{-3+8\sin^2(p_0)/\omega^2(2p_0)\}\ . \tag{15d}$$

Equation (15b) holds for the second derivative of $\omega_0^2$ taken at the critical point and this coefficient measures the curvature of the dispersion curve $\omega_0^2(p)$ near the critical point. The dispersion relation is given by Eq. (7). Furthermore, the other envelope terms are given by

$$\sin(p_0)B_1=i\left[\cos(p_0)-\left[\frac{d^2}{dp^2}\omega^2(2p)\right]_{p=p_0}\times\sin(p_0)/\omega^2(2p_0)\right]A_x\ , \tag{16a}$$

$$\omega^2(2p_0)B_2=4\sin^2(p_0)A^2\ , \tag{16b}$$

and they are connected with the envelope $A$. We observe that Eq. (15a) is of the Ginzburg-Landau type. We remark moreover, since the original equation is translationally invariant, then Eq. (15a) is invariant under phase change $A\rightarrow Ae^{i\theta}$. It is worthwhile mentioning that such a type of equation is universal and it describes how the amplitude of the first order deviates locally from the basic periodic homogeneous strain structure. The Ginzburg-Landau equation is usually met in fluid flow instability, convection problems, or reaction-diffusion system as well as in cellular instabilities of shell buckling, for instance.[7–9,34,35]

## V. STABILITY STUDY

The nonlinear analysis helps us to know whether or not the system is going to form steady organized patterns near the critical point and we must examine in more detail the equilibrium solutions to Eq. (15a) and investigate their stability. It is more convenient to rewrite Eq. (15a) in the normalized form

$$A_\tau-A_{XX}-A_{YY}+\bar{\lambda}A-\mu|A|^2A=0 \tag{17}$$

by using the transformations

$$X\rightarrow X/\sqrt{(\omega^2)_{pp}},\quad Y\rightarrow Y/\sqrt{\beta},\quad \text{and}\quad \tau\rightarrow\tau/\Gamma\ . \tag{18}$$

Equation (17) admits the following steady solutions:

$$A_0=0,\quad A_0=\pm\sqrt{\bar{\lambda}/\mu}\ , \tag{19}$$

which imposes that $\bar{\lambda}\mu>0$. However, the sign of $\bar{\lambda}$ is directly given by that of $\alpha-\alpha_0$ [see Eq. (13)] but $\mu$ can be either positive or negative according to Eq. (15d) and it depends especially on $p_0$. Now, we discuss the stability of these equilibrium states by substituting

$$A=A_0+a \tag{20}$$

into Eq. (17) where $a$ is a small time-dependent deviation about the equilibrium state $A_0$. We neglect the nonlinear terms in $a$ and we arrive at

$$a_\tau+(\bar{\lambda}-3\mu A_0^2)a=0\ . \tag{21}$$

A solution to Eq. (21) is then given by $a=a_0\exp(i\Omega\tau)$ and yields the dispersion relation

$$\Omega=i(\bar{\lambda}-3\mu A_0^2)\ . \tag{22}$$

We now consider the four cases represented by the possible signs of $\bar{\lambda}$ and $\mu$.

(i) $\bar{\lambda}>0$ (or $\alpha>\alpha_0$) and $\mu>0$. In this case there are two equilibrium solutions given by Eq. (19) (we do not distinguish between signs + and −). $A_0=0$ is stable while $A_0=\pm\sqrt{\bar{\lambda}/\mu}$ is unstable.

(ii) $\bar{\lambda}>0$ (or $\alpha>\alpha_0$) and $\mu<0$. There is only one equilibrium point $A_0=0$ which is still stable.

(iii) $\bar{\lambda}<0$ (or $\alpha<\alpha_0$) and $\mu<0$. We have two equilibrium points: $A_0=0$ which is unstable and $A_0=\pm\sqrt{\bar{\lambda}/\mu}$ which is now the stable solution as we can see by using the dispersion relation (22).

(iv) $\bar{\lambda}<0$ (or $\alpha<\alpha_0$) and $\mu>0$. In this case, there is no finite amplitude equilibrium, the one solution $A_0=0$ is

unstable, and the nonlinear effect appearing in Eq. (17) acts to reinforce the destabilizing tendency which occurs at the linear level.

It should be noticed that the solution bifurcation can be compared to the phase transition phenomena. Indeed, the equilibrium solutions can be rewritten as

$$A_0=0, \quad A_0=\pm\sqrt{(\alpha-\alpha_0)/\mu} \ . \tag{23}$$

Now, the nature of the bifurcation is clear and the equilibrium solution is a continuous function of the control parameter $\alpha$ when it crosses the critical value $\alpha_0$. Moreover, the bifurcation is then of the second order. (i) If $\mu>0$ the solution $A_0=0$ is unstable for $\alpha<\alpha_0$, whereas for $\alpha>\alpha_0$ it is also unstable. (ii) If $\mu<0$, for $\alpha<\alpha_0$ the finite equilibrium solution $A_0$ is then stable. For $\alpha>\alpha_0$ the equilibrium solution $A_0=0$ is stable. The different cases are sketched in Fig. 5, which represents the equilibrium solution $A_0$ as a function of the control parameter $\alpha$ or the elastic coefficient; this is the bifurcation diagram.

Until now, we have been interested in the homogeneous solution to Eq. (17); we now intend to study the stability of solutions to Eq. (17) in the general case of space-time-dependent amplitudes. In order to examine the linear stability, it is convenient to look for complex amplitude $A(X,Y,\tau)$ in terms of a real amplitude $\rho(X,Y,\tau)$ and phase $\theta(X,Y,\tau)$,

$$A=\rho e^{i\theta} \ . \tag{24}$$

We substitute the solution (24) into Eq. (17) and separate the real and imaginary parts to yield

$$\rho_\tau-\rho_{XX}-\rho_{YY}+\rho(\theta_X^2+\theta_Y^2+\bar{\lambda}-\mu\rho^2)=0 \ , \tag{25a}$$

$$\rho(\theta_\tau-\theta_{XX}-\theta_{YY})-2(\rho_X\theta_X+\rho_Y\theta_Y)=0 \ . \tag{25b}$$

Since the attention is focused on the transverse instabilities, we look for a solution to Eqs. (25a) and (25b) with a phase as a function of the $Y$ coordinate

$$A=\rho_0 e^{iKY} \ , \tag{26}$$

such that $\rho_0$ and $K$ are related by the equation

$$K^2+\bar{\lambda}-\mu\rho_0^2=0 \ . \tag{27}$$

Moreover, we assume that the bifurcation is normal, that is, the control parameter $\bar{\lambda}$ is negative. This also means that the linear perturbation is unstable (see Sec. III). But the coefficient $\mu$ of the nonlinear term in Eq. (17) can be either positive or negative [see Eqs. (15d)].

The linear stability analysis of the stationary transverse perturbation (26) can be readily studied by setting

$$\rho=\rho_0+a, \quad \theta=KY+b \ , \tag{28}$$

where $a$ and $b$ are small amplitude and phase perturbations and are functions of $Y$ and $\tau$. The linearization in $a$ and $b$ of Eqs. (25a) and (25b) gives

$$a_\tau-a_{YY}+(K^2+\bar{\lambda}-3\mu\rho_0^2)a+2\rho_0 K b_Y=0 \ , \tag{29a}$$

$$-2Ka_Y+\rho_0(b_\tau-b_{YY})=0 \ . \tag{29b}$$

By searching for harmonic solutions of the form $\exp[i(QY-\Omega\tau)]$ to the above equations, we arrive at the dispersion relation

$$(Q^2-i\Omega)^2-2(K^2+\bar{\lambda})(Q^2-i\Omega)-4K^2Q^2=0 \ , \tag{30}$$

where the wave number $K$ is defined by Eq. (27) and $\Omega$ and $Q$ are the frequency and wave number of the transverse disturbances. The stability of the stationary solution is guaranteed if the roots of Eq. (30) are such that $\mathrm{Im}(\Omega)<0$ for any $Q$'s. For the first root $\Omega_-$, $\mathrm{Im}(\Omega_-)$ is always negative, but for the other root

$$\Omega_+=i[K^2+\bar{\lambda}-Q^2+\sqrt{(K^2+\bar{\lambda})^2+4K^2Q^2}] \tag{31}$$

the imaginary part can be either positive or negative according to the value of $Q$. Consequently, the instability of the stationary solution with respect to the transverse disturbances occurs whenever

$$Q^2<2(\bar{\lambda}+3K^2) \ . \tag{32}$$

The condition (32) implies that $K^2>-\bar{\lambda}/3$. Figure 6 shows the imaginary part of the root $\Omega_+$ as a function of the wave number $Q$ for a negative and positive value of $\mu$. We notice that, since $\bar{\lambda}$ is rather small as well as $K$, the instability takes place for long-wavelength modulations. The condition (32) informs us about the region of wave-

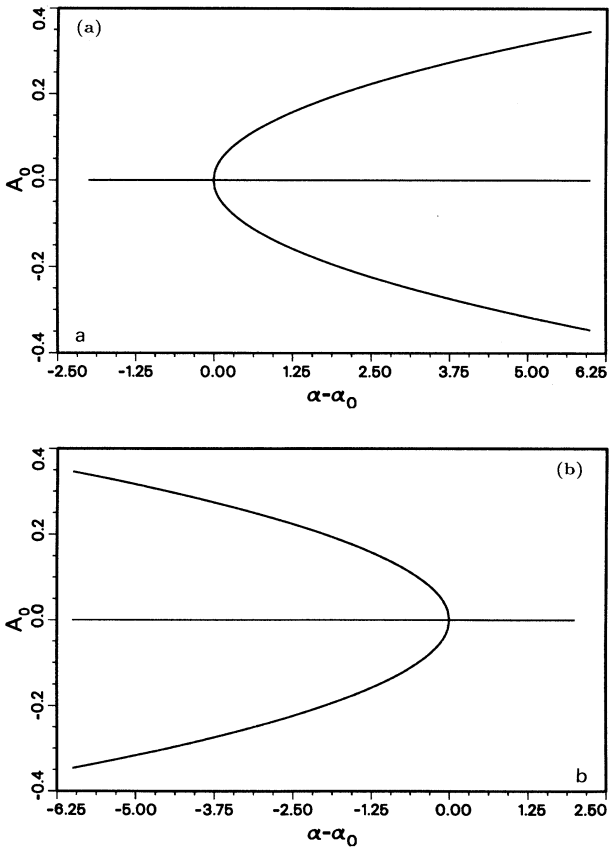


FIG. 5. The bifurcation diagram, the amplitude of the equilibrium solution as a function of the lattice force difference $\alpha-\alpha_0$ for (a) $\mu>0$ and (b) $\mu<0$.

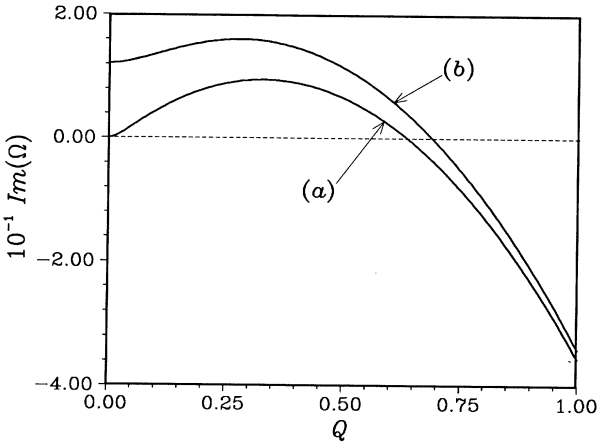


FIG. 6. The imaginary part of the frequency spectrum of the transverse disturbance as a function of the transverse wave number $Q$ for (a) $\mu<0$ (the curve passes through zero) and (b) $\mu>0$. The positive maximum of $\mathrm{Im}(\Omega)$ corresponds to the maximum of the growth rate of the transverse instability.

length selection for the transverse pattern formation. The maximum growth rate is then given by the positive maximum of Eq. (31) as depicted in Fig. 6. This analytical study allows us to understand under which conditions the pattern formation occurs at the birth of the transverse instability but the nature of the nonlinear structure emerging from the instability can only be investigated by means of numerical experiments. This will be the purpose of the following section.

## VI. NUMERICAL INVESTIGATIONS

Here, we are interested in looking for the self-organization of nonlinear structures emerging from the instability process which has been studied in the preceding section. Nevertheless, the amplitude equation (15a) informs us about the dynamics of the system at the birth of the instability process but it does not give any information concerning the long-time evolution of the system. The aim of this section is to characterize the qualitative nature of the pattern formation and its evolution in time. We undertake this task by means of numerical simulations performed directly on the microscopic system [see Eqs. (5) and (6) written in terms of the displacement $u(i,j)$]. We consider a lattice made of $121\times77$ particles; the boundary conditions are periodic on the lower and upper sides and on the right and left boundaries as well. The initial condition is simply a spatially sinusoidal deformation in the $x$ direction and homogeneous in the transverse direction as shown in Fig. 7(a). Moreover, the initial condition is a static modulation. We choose the wavelength of the periodic structure in order to have eight periods within $x$ direction so that the wavelength is 15.125 and the wave number corresponds to that of the critical one and $p_0=0.415$. Consequently, the elastic constant $\alpha$ and noncentral interaction parameter $\eta$ are computed for a given $\delta$ in order to fit with those of the critical point. Then, we obtain $\alpha_0=0.0398$, $\delta=2.4$, and $\eta=-0.1796$. For the elastic modulus $\beta$ we take $\beta=0.038$. Note that these numerical values are compatible with those used in a previous study for one- and two-dimensional models.[17,19] In order to place the system in the unstable regime, the elastic constant or lattice force $\alpha$ is slightly decreased below the critical value $\alpha_0$, such that $\alpha_0-\alpha\simeq10^{-5}$. The amplitude of the initial strain modulation is rather small, $\rho_0=0.0165$. Shortly later, small perturbations are taking place along the transverse direction but the periodic strain structure remains static as the initial condition. This situation is shown in Fig. 7(b). The instabilities are growing whereas the height strain bands are still static. After a lapse of time, the instabilities produce localized structures along the transverse direction as depicted in Fig. 7(c). We can observe very clearly, for each strain band, five ellipse-shaped structures.

A rough computation of the transverse instability from Eqs. (27) and (31) leads to $K\simeq0.0694$ and the maximum growth rate occurs at $Q_{\max}\simeq0.308$ so that the transverse wave number selected by the instability process is $K+Q_{\max}\simeq0.3774$. The latter value can be compared to that observed on the computerized picture [see Fig. 7(c)], then the wavelength of the transverse modulations is $\lambda\simeq15.4$ corresponding to the wave number $Q\simeq0.4$, which is of the same order. The small discrepancy (6%) is due to the periodic boundary condition in the transverse direction, indeed, we must have an integer number of periods within the transverse length of the lattice. By continuing the numerical simulation a little bit longer, we can notice that the instability growth leads to the movement of the localized structures. These structures merge and form a bigger band with localized strain domains on the left of Fig. 7(d) whereas the localized patterns on the right are vanishing. Afterwards, the structures are transformed into a strain band which is modulated along the transverse direction, but three bands of disk-shaped domains are still present on the right [see Fig. 7(e)]. After a lapse of time, the strain band becomes larger almost homogeneously in the $y$ direction at the expense of some localized structures which are dying down as depicted in Fig. 7(f). Nevertheless, the pattern thus obtained evolves to a stationary state made of a rather large homogeneous strain band as plotted in Fig. 7(g). In fact, such a structure can be considered as a solution to the one-dimensional (in the $x$ direction) model.[16,19] In addition, the numerics provides the total energy of the system and it can be shown that the energy decreases with some oscillations and finally stays constant. This proves that the system has reached its stationary state. This numerical investigation ascertains first the occurrence of the transverse instability of a strain modulation near the instability point of the acoustic branch of dispersion, and secondly the nature and stability of the nonlinear structure emerging from the instability process modeled by the amplitude equation (15).

## VII. CONCLUSIONS

Our main objective was merely to describe the physical mechanisms of nonlinear structure formation occurring

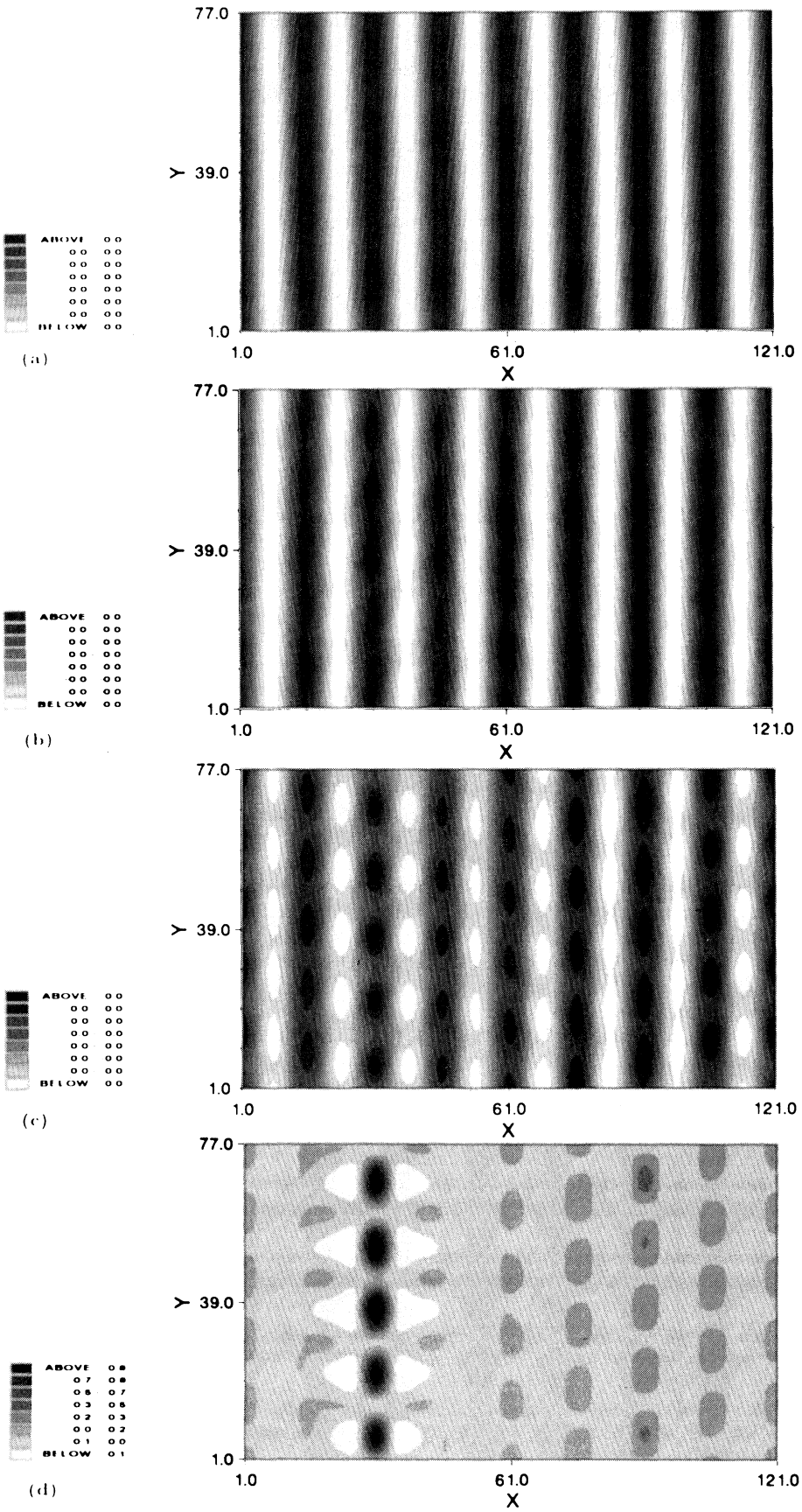


FIG. 7. Instability mechanism of a periodic strain structure on a two-dimensional lattice: (a) the initial condition is a strain modulation homogeneous in the $y$ direction, (b) transverse perturbations are wrinkling along the $y$ direction, (c) formation of localized structures within the strain modulation along the transverse direction, (d) the periodic structure breaks and a strain band with disk-shaped domains is formed, (e) modulated-strain band and vanishing localized patterns, (f) formation of a strain band on the left, some localized structures on the right are dying down, and (g) the long-time evolution of the system: stationary state made of a homogeneous strain band.

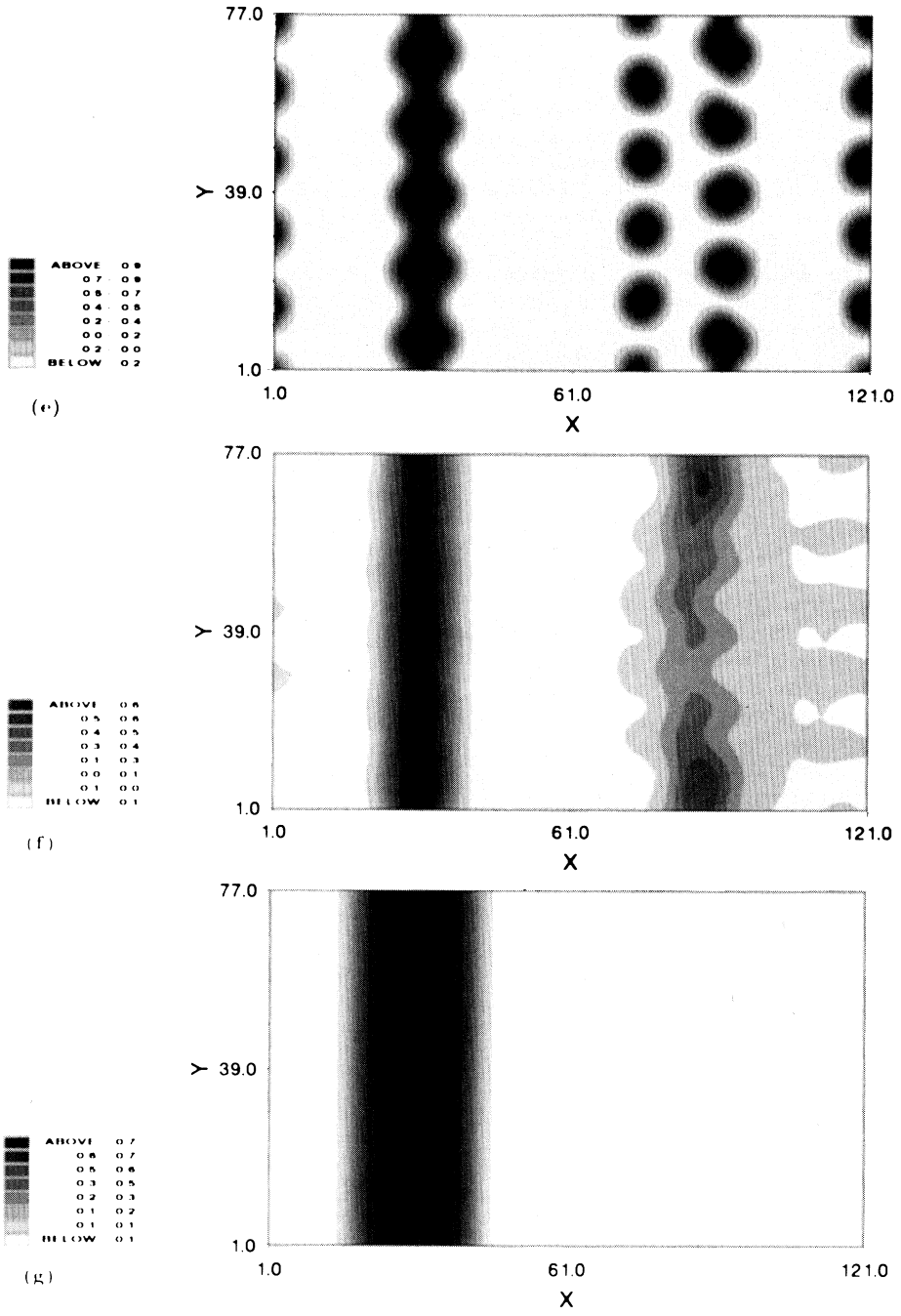


FIG. 7. (*Continued*).

for ferroelastic transitions at the instability point of the phonon dispersion on the basis of a two-dimensional lattice model. The pattern formation is interpreted here as the nucleation and growth of ferroelastic domains triggered by instability of modulated-strain structures or strain modulation taking place at the pretransformation point. The fundamental phenomenon is the existence of lattice instability due to the low softening of the transverse-acoustic branch of dispersion at a nonzero wave number. The latter corresponds to the spatial period of the strain modulation developing in alloys such as Fe-Pd, Ni-Al, and others. These effects are characterized by microtexture formation made of fine-scale arrangements of modulated-strain domains which are usually observed by high-resolution electron microscopy.[13,14] By using multiple-scale technique in the vicinity of the critical point we have obtained, in the semidiscrete approach, an amplitude equation of the Ginzburg-Landau type. The discrete part of the solution to the microscopic system is, in fact, provided by the linear analysis near the critical point of the acoustic branch of dispersion while the envelope term is considered in the long-wavelength

limit. Moreover, the discrete part of the solution describes the static strain modulation of the lattice. The envelope equation [see Eq. (15)] allows us to examine the stability of the basic stationary solution; this is done in Sec. V. Then, it is proved that the transverse instability occurs for the long-wavelength modulations given by the criterion (32) when the bifurcation is normal. The study of stability tells us under which conditions the transverse structure birth can take place. However, thanks to the numerical investigations we can clarify the nature of the nonlinear structures on the two-dimensional lattice. In fact, we obtain a self-localization of the transverse instabilities in a two-dimensional periodic spatial structure. The pattern thus obtained is interpreted as the formation or nucleation of lenticular or ellipse-shaped twins consisting of a two-dimensional array of ferroelastic domains growing in the high-temperature phase (paraelastic phase). However, these localized patterns are metastable states corresponding to a local minimum of the total energy of the lattice. That means that the system must evolve toward an absolute minimum of which the stationary state is characterized by a homogeneous strain band [see Figs. 7(a)–7(g)]. The instability mechanism can be seen as the nucleation of a ferroelastic domain within the high-temperature phase (or the martensite on an austenic phase). These complex structures are commonly observed on electron micrographs for various alloys.[36,37] We would like to point out that the present work is somewhat similar to that of the well-known hydrodynamic instability in fluid mechanics or reaction-diffusion systems exhibiting dissipative or spatiotemporal structures,[7–9] but the physical background is quite different.[38]

On the other hand, the present study provides insight into the understanding of the phase transformation in alloys especially for martensitic-ferroelastic transformations and it is concerned especially with pretransformation effects or precursory phase. The model is also suited to the commensurate-incommensurate phase transition for which the dynamics of topological defect are particularly important.[3] This happens when the spatial period of the strain modulation is not a multiple of the lattice period. This interesting problem can be envisaged in another work. In addition, the influence of an applied field and damping on the dynamics of the nonlinear structure formation is worth studying in the framework of nonequilibrium physics. The problem of the behavior of the very discrete model without considering the continuum approximation can be undertaken by introducing a substrate potential involving multistable minima which characterize the possible variants of ferroelastic phases. At this stage the model must include two displacement components. Some aspects of these further problems are presently under study.

## ACKNOWLEDGMENT

The Laboratoire de Modélisation en Mécanique is "Unité Associée au Centre Nationale de la Recherche Scientifique."

[1]A. V. Gaponov-Grekhov and M. I. Rabinovich, Phys. Today **43**(7), 30 (1990).
[2]F. Falo, A. R. Bishop, P. S. Lomdahl, and B. Horovitz, Phys. Rev. B **43**, 8081 (1991).
[3]K. Parlinski, F. Denoyer, and G. Eckold, Phys. Rev. B **43**, 8411 (1991).
[4]M. B. Salamon, M. E. Meiche, and C. M. Wayman, Phys. Rev. B **31**, 7306 (1985).
[5]S. M. Shapiro, in *Competing Interactions and Microstructures: Statics and Dynamics*, edited by R. Lesar, A. R. Bishop, and R. Heffner, Springer Proceedings in Physics Vol. 27 (Springer-Verlag, Berlin, 1988), pp. 84–94.
[6]L. E. Tanner, D. Schryvers, and S. M. Shapiro, Mater. Sci. Eng. A **127**, 205 (1990).
[7]D. Walgraef, Solid State Phenomena **3&4**, 77 (1988).
[8]P. Coullet and P. Huerre, Physica D **23**, 27 (1986).
[9]M. C. Cross, P. G. Daniels, P. C. Hohenberg, and E. D. Siggia, J. Fluid Mech. **127**, 155 (1983).
[10]J. A. Krumhansl and R. J. Gooding, Phys. Rev. B **39**, 3047 (1989).
[11]K. Fuchizaki and Y. Yamada, Phys. Rev. B **40**, 4740 (1989).
[12]G. R. Barsch and J. A. Krumhansl, Metall. Trans. **19A**, 761 (1987).
[13]K. M. Knowles, J. M. Christian, and D. A. Smith, J. Phys. (Paris) Colloq. **43**, C4-185 (1982).
[14]R. Oshima, M. Sugiyama, and F. E. Fujita, Metall. Trans. **19A**, 803 (1988).
[15]J. Pouget, in *Continuum Models and Discrete Systems 6*, edited by G. A. Maugin (Longman Scientific and Technical, London, 1991), pp. 296–312.
[16]J. Pouget, Phase Transitions **34**, 105 (1991).
[17]J. Pouget, Phys. Rev. B **46**, 10 554 (1992).
[18]J. Pouget, Phys. Rev. B **43**, 3575 (1991).
[19]J. Pouget, Phys. Rev. B **43**, 3582 (1991).
[20]K.-M. Ho, C. L. Fu, and B. N. Harmon, Phys. Rev. B **29**, 1575 (1984).
[21]Y. Noda, Y. Yamada, and S. M. Shapiro, Phys. Rev. B **40**, 5995 (1989).
[22]Y. Yamada and K. Fuchizaki, Phys. Rev. B **42**, 9420 (1990).
[23]J. D. Axe and G. Shirane, Phys. Rev. B **8**, 1965 (1973).
[24]T. Finlayson, M. Mostoller, W. Reichardt, and H. G. Smith, Solid State Commun. **53**, 461 (1985).
[25]S. M. Shapiro, J. Z. Lerese, Y. Noda, S. C. Moss, and L. E. Tanner, Phys. Rev. Lett. **57**, 3199 (1986).
[26]L. E. Tanner, A. R. Pelton, and R. Gronsky, J. Phys. (Paris) Colloq. Suppl. **43**, C4-169 (1982).
[27]R. Oshima, M. Sugiyama, and F. E. Fujita, Metall. Trans. **19A**, 803 (1988).
[28]A. C. Newell and J. A. Whitehead, J. Fluid Mech. **38**, 279 (1969).
[29]F. H. Busse, Rep. Prog. Phys. **41**, 1929 (1978).
[30]E. Courtsias and B. A. Huberman, Phys. Rev. B **24**, 2592 (1981).
[31]A. Novick-Cohen, J. Stat. Phys. **38**, 707 (1985).
[32]N. Flytzanis, S. Pnevmatikos, and M. Remoissenet, J. Phys. C **18**, 4603 (1985).

[33]M. Remoissenet, Phys. Rev. B **33**, 2386 (1986).
[34]G. Iooss, A. Mielke, and Y. Demay, Eur. J. Mech. B (Fluids) **229** (1989).
[35]N. Damil and M. Potier-Ferry, Dynamics Stability Syst. **7**, 1 (1992).
[36]L. Baele, G. Van Tendeloo, and S. Amelinckx, Acta Metall. **35**, 401 (1987).
[37]D. Broddin, G. Van Tendeloo, J. Van Landuyt, and S. Amelinckx, Philos. Mag. B **57**, 31 (1988).
[38]D. Broddin, G. Van Tendeloo, J. Van Landuyt, and S. Amelinckx, Philos. Mag. A **59**, 47 (1989).

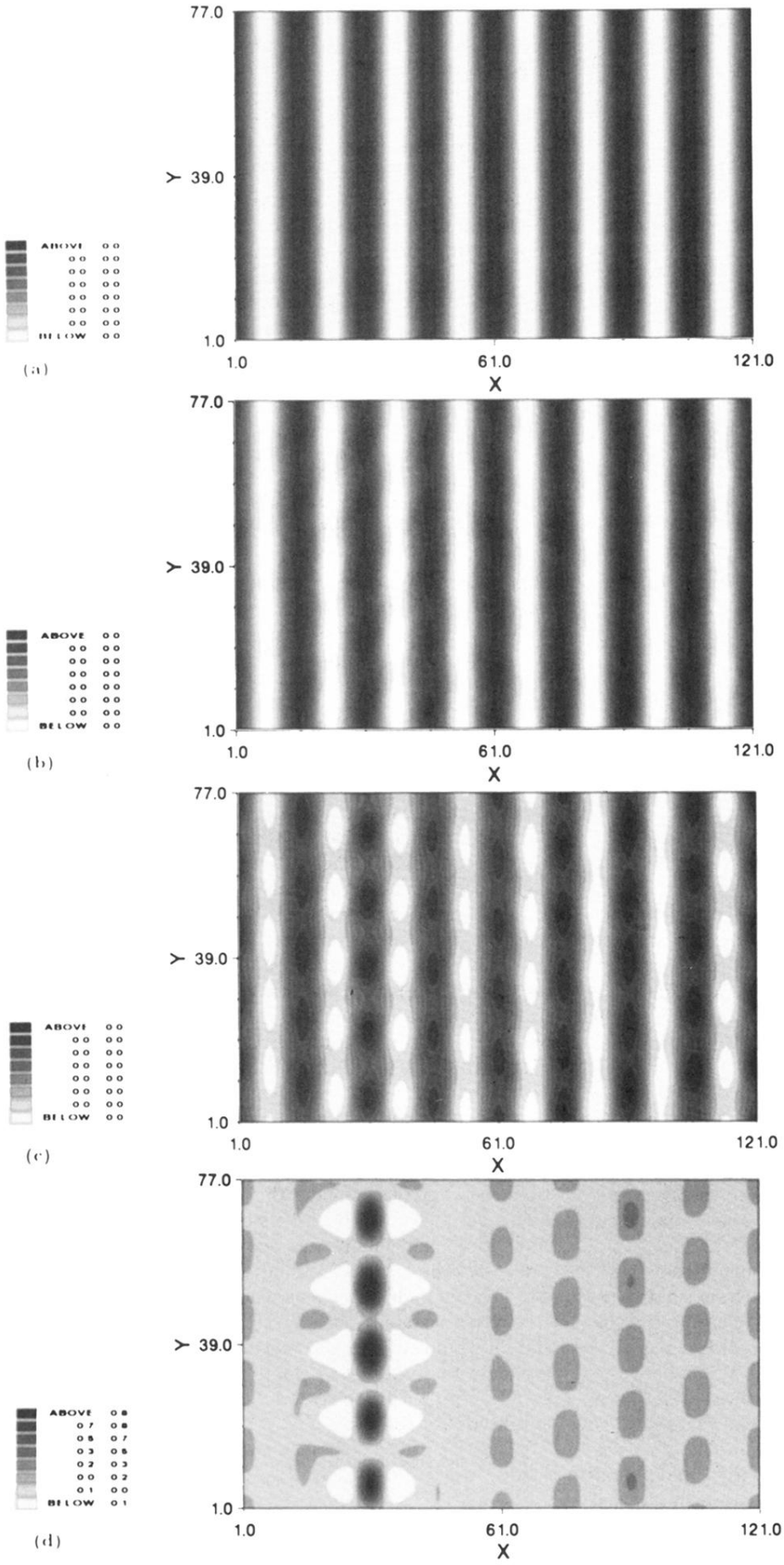


FIG. 7. Instability mechanism of a periodic strain structure on a two-dimensional lattice: (a) the initial condition is a strain modulation homogeneous in the $y$ direction, (b) transverse perturbations are wrinkling along the $y$ direction, (c) formation of localized structures within the strain modulation along the transverse direction, (d) the periodic structure breaks and a strain band with disk-shaped domains is formed, (e) modulated-strain band and vanishing localized patterns, (f) formation of a strain band on the left, some localized structures on the right are dying down, and (g) the long-time evolution of the system: stationary state made of a homogeneous strain band.

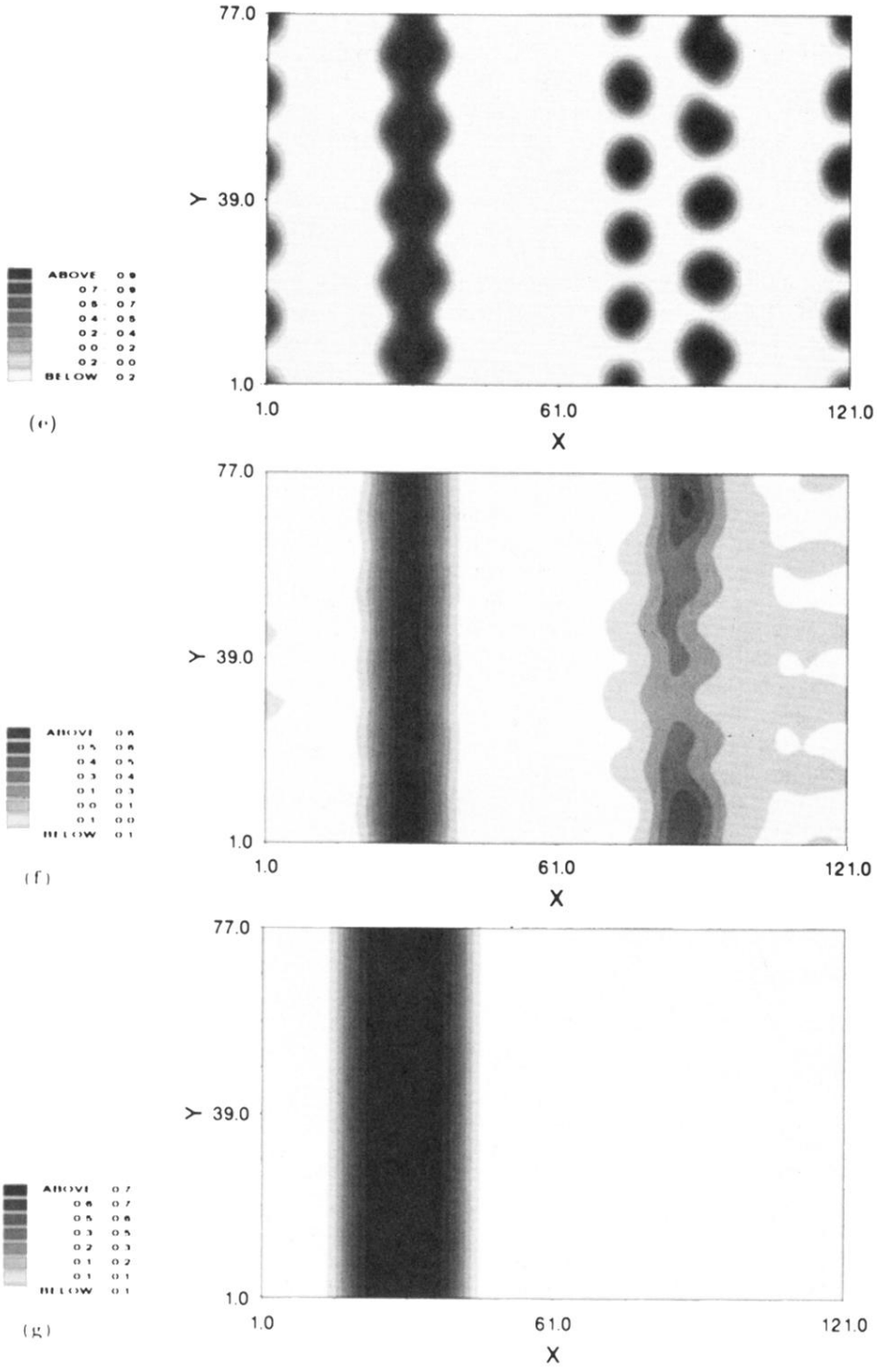


FIG. 7. (*Continued*).